

# How Lipid Headgroups Sense the Membrane Environment: An Application of $^{14}\text{N}$ NMR

Jacques P. F. Doux,<sup>†</sup> Benjamin A. Hall,<sup>†,\*</sup> and J. Antoinette Killian<sup>†</sup>

<sup>†</sup>Membrane Biochemistry and Biophysics, Bijvoet Center for Biomolecular Research, Utrecht University, Utrecht, The Netherlands; and <sup>\*</sup>Oxford Centre for Integrative Systems Biology, Department of Biochemistry, Oxford, United Kingdom

**ABSTRACT** The orientation of lipid headgroups may serve as a powerful sensor of electrostatic interactions in membranes. As shown previously by  $^2\text{H}$  NMR measurements, the headgroup of phosphatidylcholine (PC) behaves like an electrometer and varies its orientation according to the membrane surface charge. Here, we explored the use of solid-state  $^{14}\text{N}$  NMR as a relatively simple and label-free method to study the orientation of the PC headgroup in model membrane systems of varying composition. We found that  $^{14}\text{N}$  NMR is sufficiently sensitive to detect small changes in headgroup orientation upon introduction of positively and negatively charged lipids and we developed an approach to directly convert the  $^{14}\text{N}$  quadrupolar splittings into an average orientation of the PC polar headgroup. Our results show that inclusion of cholesterol or mixing of lipids with different length acyl chains does not significantly affect the orientation of the PC headgroup. In contrast, measurements with cationic (KALP), neutral (Ac-KALP), and pH-sensitive (HALP) transmembrane peptides show very systematic changes in headgroup orientation, depending on the amount of charge in the peptide side chains and on their precise localization at the interface, as modulated by varying the extent of hydrophobic peptide/lipid mismatch. Finally, our measurements suggest an unexpectedly strong preferential enrichment of the anionic lipid phosphatidylglycerol around the cationic KALP peptide in ternary mixtures with PC. We believe that these results are important for understanding protein/lipid interactions and that they may help parametrization of membrane properties in computational studies.

## INTRODUCTION

Interactions between membrane proteins and surrounding lipids are of key importance for membrane structure and organization (for reviews see (2–5)). For example, the lipid composition of membranes can influence properties of proteins such as mode of membrane insertion, topology, folding, stability, dynamics, or extent of membrane binding. Vice versa, membrane proteins can influence the structure, lateral organization, and dynamics of membrane lipids. However, understanding the precise molecular nature of these protein/lipid interactions remains a challenge.

Membrane proteins often contain positively charged residues, such as lysines, histidines, and arginines that are located at the lipid water interface (6,7). In many cases electrostatic interactions, mediated via these positive charges on the proteins and the polar headgroup of the lipids, play an important role in protein/lipid interactions. To better understand the potential consequences of electrostatic interactions on a molecular level, we focus on how the lipid headgroups sense the presence of charges on membrane-embedded proteins.

Several studies already have shown that the polar headgroup orientation is sensitive to charges in its vicinity (1,8–15). Using deuterium NMR on phosphatidylcholine (PC) that was specifically labeled at the  $\text{C}_\alpha$  and  $\text{C}_\beta$  carbons

of the choline moiety of the headgroup, Seelig and co-workers (1,8) showed that introduction of negatively charged lipids leads to a more parallel orientation of the P-N dipole of the PC headgroup with respect to the membrane surface, whereas incorporation of cationic lipids drives the positively charged end of the dipole further away from the membrane surface toward the aqueous phase, leading to a more perpendicular orientation. This was introduced as the electrometer concept (8). The introduction of deuterium labels is an elegant approach, because the labels are sensitive reporters that do not interfere with biophysical interactions. Nevertheless, the method has the drawback of requiring chemical synthesis of labeled lipids. Therefore, other groups explored the idea of gaining similar insights using  $^{14}\text{N}$  NMR (8,16–19). This isotope is almost 100% naturally abundant in PC, and as with deuterium, the NMR response is related to the orientation of the surrounding electric field gradient relative to the magnetic field. However, most likely due to its low sensitivity, the method has not been widely applied.

With progress in modern instrumentation and the need for simple methods to study the interactions in the polar head region, the application of  $^{14}\text{N}$  NMR recently has regained interest (20–22). Here, we explore the use of  $^{14}\text{N}$  NMR to study electrostatic interactions at the membrane surface by systematically analyzing effects of introducing positively and negatively charged lipids on the headgroups of the surrounding lipids. In addition, the effect of incorporating transmembrane peptides was studied. These peptides consist of  $\alpha$ -helical stretches of varying length, flanked on both

Submitted May 10, 2012, and accepted for publication August 10, 2012.

\*Correspondence: benjamin.a.hall@ucl.ac.uk

Benjamin A. Hall's present address is Centre for Computational Science, Department of Chemistry, University College London, London, UK.

Editor: Francesca Marassi.

© 2012 by the Biophysical Society  
0006-3495/12/09/1245/9 \$2.00

<http://dx.doi.org/10.1016/j.bpj.2012.08.031>

sides either by two positive Lys residues (KALP), by two His of which the charge can be controlled by pH (HALP), or by acetylated Lys as a neutral control (Ac-KALP). These peptides have been extensively studied and they make excellent tools to approach complex phenomena in a systematic way (23–27).

The results show that by using  $^{14}\text{N}$  NMR on our model systems it is possible to detect subtle changes in headgroup orientation as a consequence of electrostatic interactions. In particular, very systematic changes were found in response to the presence of charged peptide side chains near the interface. These results will be discussed in light of recent literature data on the importance of electrostatic interactions for protein/lipid interactions in membranes.

## MATERIALS AND METHODS

### Materials

All phospholipids were purchased from Avanti Polar Lipids (Alabaster, AL). These lipids included 1,2-dilauroyl-*sn*-glycero-3-phosphocholine (DLPC), 1,2-dimyristoyl-*sn*-glycero-3-phosphocholine (DMPC), 1,2-dipalmitoyl-*sn*-glycero-3-phosphocholine (DPPC), 1,2-dimyristoleoyl-*sn*-glycero-3-phosphocholine (14:1PC), 1,2-dipalmitoleoyl-*sn*-glycero-3-phosphocholine (16:1PC), 1,2-dioleoyl-*sn*-glycero-3-phosphocholine (DOPC or 18:1PC), 1,2-dieicosenoyl-*sn*-glycero-3-phosphocholine (20:1PC), 1,2-dierucoyl-*sn*-glycero-3-phosphocholine (22:1PC), 1,2-dimyristoyl-3-trimethylammonium-propane (DMTAP), and 1,2-dimyristoyl-*sn*-glycero-3-phospho-(1'-rac-glycerol) (DMPG). Cholesterol (>99% purity), chloroform, methanol, and 2,2,2-trifluoroethanol (TFE) were obtained from Sigma-Aldrich Chemie B.V. (Zwijndrecht, Netherlands). Water was deionized and filtered with a Milli-Q water purification system from Millipore (Billerica, MA). HALP23 [Ac-GHHL(Al)<sub>8</sub>HHA-NH<sub>2</sub>] and KALP23 [Ac-GKKL(Al)<sub>8</sub>KKA-NH<sub>2</sub>] were synthesized via solid phase peptide synthesis as previously described (28), purified with reversed phase high-performance liquid chromatography to >90% purity and identified by mass spectrometry.

### Preparation of Ac-KALP23

The lysines of KALP23 were acetylated by dissolving 40 mg of purified KALP23 in a mixture of an excess of acetic anhydride (70  $\mu\text{l}$ ) with *N,N*-diisopropylethylamine (70  $\mu\text{l}$ ) in 2 ml chloroform with 35  $\mu\text{l}$  of dimethylformamide. The reaction mixture was stirred at room temperature for 1 h. The resulting peptide (Ac-KALP23) was then precipitated in cold methyl *t*-butyl ether/*n*-hexan (1:1 by volume) and sedimented by centrifugation. The pellet was resuspended in tert-butanol/water 1:1 (by volume) and freeze-dried. MALDI-TOF mass spectrometry showed complete acetylation of the peptide with only one peak at 2480 *m/z*, corresponding to the expected mass of the [M+Na<sup>+</sup>] ion.

### Sample preparation

The concentration of peptide stock solution in TFE (around 6 mM) was determined using ultraviolet absorption at 214 nm in TFE according to (29). The extinction coefficients used were 21184 M<sup>-1</sup>cm<sup>-1</sup> for KAL23, 24876 M<sup>-1</sup>cm<sup>-1</sup> for Ac-KALP23, and 41520 M<sup>-1</sup>cm<sup>-1</sup> for HALP23. The concentration of lipid stock solutions (in chloroform for PC and in chloroform/methanol 1:1 (by volume) for proteoglycan (PG)) was determined by their phosphate content according to Rouser et al. (30). The concentration of DMTAP stocks (around 50 mM) was solely determined by weight. Mixtures of lipids and peptides were cosolubilized at the desired

molar ratio in glass tubes. They were dried under a nitrogen stream yielding thin films. Organic solvents were further evaporated under vacuum for at least 2 h. The lipid films were then hydrated at 40°C using 1 ml of Mili-Q water and subjected to 3 to 10 freeze-thaw cycles. The milky emulsion was then transferred to 1.5 ml Eppendorf tubes and freeze-dried overnight. The powder was hydrated at 50% weight total with Mili-Q water, and allowed to equilibrate for about a day at 37°C. The pH was checked with paper strips and was found to be between 6.4 and 7. For samples containing HALP23 the pH was adjusted with either HCl or NaOH. After equilibration, the mixture was transferred by centrifugation to a 4 mm outer diameter ZrO<sub>2</sub> tube closed with a Kel-F cap. The samples were stored at 4°C before the measurements.

### NMR experiments

The NMR measurements were carried out on a Bruker (Rheinstetten, Germany) wide bore Ultrashield magnet of 11.7 T with an Avance 500 console recently upgraded to Avance III. A broadband double channel probe was used with interchangeable antennas. The  $^{31}\text{P}$ -NMR was carried out at a frequency of 202.5 MHz applying a standard Hahn echo ( $\pi/2 - \tau - \pi - \tau$  - acquisition) with proton decoupling using a 5  $\mu\text{s}$   $\pi/2$  pulse, a 50  $\mu\text{s}$  echo delay, and a 1.5 s recycling delay. The spectral width was 250 ppm and the temperature was 40°C. For the  $^{14}\text{N}$ -NMR measurements, the lower frequency of the probe, which was originally limited to  $^{15}\text{N}$  was tuned down to the 36.1 MHz frequency using a homemade self-supported 4 mm inner diameter copper solenoid antenna. The  $^{14}\text{N}$ -NMR experiments were carried out at variable temperatures ranging from 10 to 90°C. The pulse sequence was a standard solid echo sequence ( $\pi/2 - \tau - \pi/2 - \tau$  - acquisition) using a 300 ms recycling delay, an 80  $\mu\text{s}$  echo delay, and a 4.2  $\mu\text{s}$  pulse duration. The spectral width was 500 kHz, and the acquisition time was 2 ms resulting in a free induction decay resolution of 250 Hz. The spectra were zero-filled (31) and multiplied with a 200 Hz decaying exponential before Fourier transformation. To extract the  $^{14}\text{N}$  quadrupolar splittings from the powder spectra, they were fitted using the solid line shape analysis routine from Bruker Topspin 3 software. This allows high accuracy even with slightly noisy data.

### Estimation of headgroup orientation from $^{14}\text{N}$ quadrupolar splittings

$^{14}\text{N}$  has a spin  $I = 1$  and in an anisotropic medium the spectrum will exhibit a quadrupolar splitting. The  $^{14}\text{N}$  quadrupolar tensor is axially symmetric. Hence, this quadrupolar splitting is a direct measurement for the molecular order parameter of the C $_{\beta}$ -N (CN) bond of the choline moiety with respect to the magnetic field. As lipids undergo rapid rotations, this order parameter is further averaged symmetrically. The frequency separation between the two peaks in the powder spectrum is given by

$$\Delta\nu = \frac{3}{4} \frac{e^2qQ}{h} S_{\text{mol}} \frac{3 \cos^2(\theta) - 1}{2}, \quad (1)$$

where  $e^2qQ/h = 135$  kHz is the nitrogen quadrupole coupling constant (31,32),  $S_{\text{mol}}$  the intermolecular order parameter that accounts for motional averaging, and  $\theta$  is the time and space averaged angle of the CN vector with respect to the magnetic field.

From Fig. 1 it is clear that we can decompose  $\theta = \varphi + \delta$  where  $\varphi$  is the phosphorous-nitrogen (PN) direction and  $\delta$  is the angle between the CN and PN vectors. Previously, Semchyschyn and Macdonald (33) determined the orientation of the PN vector as a response to surface charge by combining results from multiple NMR variables. These included quadrupolar splittings from C $_{\alpha}$ -d<sub>2</sub>, C $_{\beta}$ -d<sub>2</sub>, and C $_{\gamma}$ -d<sub>9</sub> deuterated lipids, dipolar splittings from  $^{13}\text{C}_{\alpha}$  and  $^{13}\text{C}_{\alpha}$ - $^{13}\text{C}_{\beta}$ -labeled POPC and the residual chemical shift anisotropy from  $^{31}\text{P}$ . In these studies no  $^{14}\text{N}$  quadrupolar splittings were measured. However, because the charge densities were the same as those used in this study, it is possible to combine the PN angles described in Fig. 12 of

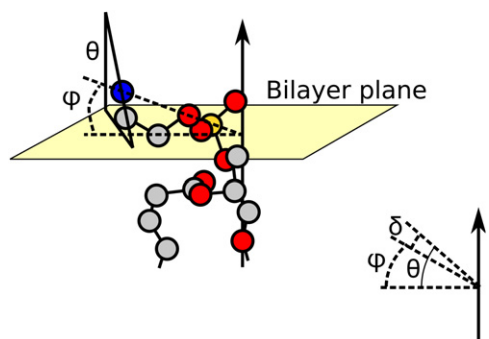


FIGURE 1 Schematic representation of the angles  $\theta$ ,  $\phi$ , and  $\delta$  where  $\phi$  is the PN direction and  $\delta$  is the angle between the CN and PN vectors of the PC headgroup. The  $\gamma$ -methyl groups of the choline are removed for clarity of the angle definitions. For details see text.

(33) as abscissa with the quadrupolar splittings found in this study as ordinate, and to determine  $\delta$  and  $S_{\text{mol}}$  from these values by fitting Eq. 1. Once parametrized, Eq. 1 can be used to approximate the orientation of the PN vector for any sample. Although in principle four angles could give rise to the same magnitude of quadrupolar splittings, this can be reduced to only one angle, based on the known geometry of the choline headgroup. Using the nonlinear least square fitting routine of Gnuplot (34) at 40°C we found  $\delta = -11.1 \pm 1.3^\circ$  and  $S_{\text{mol}} = 0.119 \pm 0.003$ . This small value of  $S_{\text{mol}}$  suggests a strong dynamics of the polar head, consistent with previous findings (19). The final fit is illustrated in Fig. 2. It is important to note that these angles of the P-N vector orientation are purely indicative. As Semchyschyn and Macdonald (33) showed, all torsion angles of the choline headgroup change with the electrometer response, and therefore it is not a simple hinge motion around the phosphate group. However, we believe that any additional corrections mainly would result in a small offset of the data, and thus would not affect the main conclusions from our study.

## RESULTS AND DISCUSSION

### Validating the method: the electrometer concept

Both phosphorous and nitrogen are present in the polar head of PC, making them ideal isotopes to study the orientation of

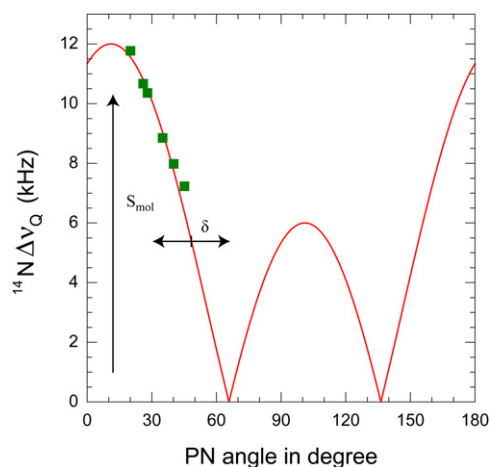


FIGURE 2 Fit of Eq. 1 to the calculated P-N angles of the lipid headgroup with the membrane surface from Semchyschyn and Macdonald (33) and the corresponding values of the  $^{14}\text{N}$  quadrupolar splittings in this study.

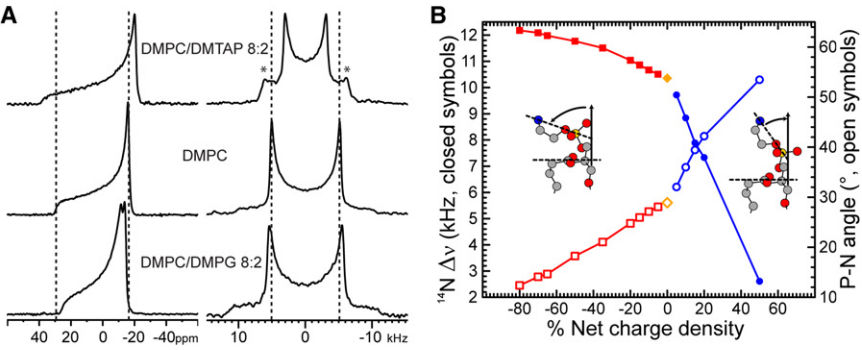
the choline moiety with respect to the bilayer plane by NMR methods. Fig. 3 illustrates their sensitivity to the presence of charge in their vicinity. The left-hand side of A represents typical  $^{31}\text{P}$  NMR spectra of DMPC in the absence and presence of charged amphiphiles. The spectra are all axially symmetric with a low field shoulder and a high field peak, characteristic for a bilayer organization. The residual chemical shift anisotropy (CSA) is  $\sim 42$  ppm in DMPC (middle), but slightly increases upon addition of the positively charged DMTAP (top) and slightly decreases upon incorporation of the negatively charged DMPG (bottom). DMPG has a slightly smaller CSA than DMPC (35) and therefore it shows up as an additional peak at a slightly lower field.

The  $^{14}\text{N}$  spectra on the right-hand side of Fig. 3 A shows the opposite trend. The spectra are again axially symmetric with a quadrupolar splitting of 10.38 kHz for DMPC (middle), which now decreases upon incorporation of DMTAP (top), but increases upon incorporation of DMPG (bottom). These results are fully consistent with previous findings by  $^2\text{H}$ -NMR from Seelig and co-workers (1,8) on the electrometer concept. For further analysis of the behavior of the headgroup we focused on the  $^{14}\text{N}$  quadrupolar splittings, because they are relatively straightforward to analyze in terms of a time average orientation of the N- $\text{C}_\beta$  bond, due to the geometry and motion of the  $^{14}\text{N}$  tensor. In contrast, the  $^{31}\text{P}$  CSA is quite complex to analyze, as it is not only sensitive to orientation and motion but also can be affected by neighboring molecules that influence the shielding of the nucleus.

The quadrupolar splittings were measured as a function of the concentration of DMTAP and DMPG and plotted as a function of charge density in Fig. 3 B. It is clear from this figure that the splittings are very sensitive to the presence of positive charges, but much less so to the presence of negative charges. Also shown in this figure are the corresponding values of the PN-orientation with respect to the surface charge, calculated as described in the Materials and Methods. The inset illustrates the direction of motion of the headgroup: upon introducing negative charges the headgroup moves toward the membrane surface, and upon introducing positive charges the headgroup moves away from the surface.

### Temperature-dependent measurements allow discrimination between motion and orientation

The  $^{14}\text{N}$  quadrupolar splittings as measured in Fig. 3 B are determined both by the orientation and by dynamical properties of the lipid headgroups. Because temperature will affect thermal motions, it will affect the dynamical parameter. In addition, temperature may affect the average orientation of the headgroup. The upper panel of Fig. 4 represents the quadrupolar splittings of the choline moiety in the presence of charged amphiphiles as a function of temperature (see also Table 1). Each trace has the same features, a sharp



with the bilayer plane of the P-N vector calculated using the model and parameters described in the Material and Methods. The inset schematically represents the behavior of the polar headgroup as determined by Sherer and Seelig (8) or Semchyschyn and Macdonald (33). The  $\gamma$ -methyl groups of the choline are removed for clarity.

decrease of the quadrupolar splitting near the gel to a liquid-crystalline phase transition of the lipids, and a further linear decrease in the fluid phase. The phase transition broadens with increasing concentrations of DMTAP, as was previously observed using  $^{14}\text{N}$  NMR by Siminovitch et al. (32). A remarkable observation from this figure is that, once in the fluid phase, all the thermograms are parallel. Thus, the

headgroups most likely undergo similar temperature-dependent motional averaging with an offset due to a change in orientation of the polar head when interacting with charged molecules.

Next, we investigated to what extent the  $^{14}\text{N}$  quadrupolar splitting is sensitive to variations in lipid packing. The lower panel of Fig. 4 shows the quadrupolar splitting of different length PC lipids as a function of temperature. In all cases the splittings are clearly dependent on temperature, indicative of increasing motional averaging with increasing temperature (Table 1). However, they appear to be independent of lipid composition. When the lipids are in the fluid phase, the data in all systems overlay one another. This is even the case for a binary mixture of DLPC and DPPC, where one would expect to find some heterogeneity at the lipid/water interface. This result suggests that in mixtures of lipids with different chain length the headgroups align at the surface, whereas the acyl chains adapt to optimize their packing. Furthermore, the presence of cholesterol, which may give the headgroups more motional freedom by acting as a spacer, does not affect the quadrupolar splitting, in line with previous observations using  $^{31}\text{P}$  and  $^2\text{H}$  NMR (36). Similarly, changes in  $[\text{NaCl}]$  from 0 to 300 mM did not significantly affect the quadrupolar splitting

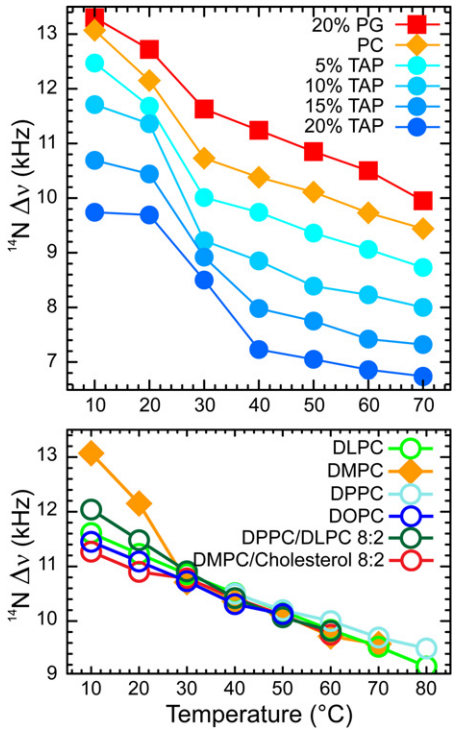


FIGURE 4 Effect of temperature on various lipid mixtures. Top panel: From top to bottom,  $^{14}\text{N}$  quadrupolar splittings of DMPC with 20 mole % DMPG (squares), DMPC (diamonds), DMPC with 5, 10, 15, 20 mole % DMTAP (circles). Lower panel:  $^{14}\text{N}$  quadrupolar splitting of various dispersions of PC with different acyl chains, of a binary mixture of DMPC/Cholesterol 8:2 and of DPPC/DLPC 8:2. N.B. DPPC is depicted only from 40–C.

**TABLE 1** Effect of temperature on the  $^{14}\text{N}$  quadrupolar splittings (in kHz) of dispersions of DMPC in the absence and presence of anionic or cationic lipids and cholesterol

Temperature (°C)	10	20	30	40	50	60	70	80
20% DMPG	13.30	12.72	11.63	11.24	10.85	10.50	9.95	—
DMPC sample 1	13.07	12.15	10.71	10.37	10.12	9.72	9.58	—
DMPC Sample2	13.07	12.15	10.73	10.38	10.11	9.73	9.44	—
5% DMTAP	12.47	11.68	10.01	9.74	9.36	9.06	8.73	—
10% DMTAP	11.71	11.36	9.22	8.85	8.39	8.23	8.00	—
15% DMTAP	10.69	10.44	8.92	7.98	7.75	7.42	7.32	—
20% DMTAP	9.74	9.69	8.50	7.23	7.05	6.86	6.74	—
50% DMTAP	—	—	—	3.84	3.93	3.98	4.05	—
DMPC+20%chol	11.27	10.90	10.78	10.42	10.11	9.75	—	—

Lipid percentages represent mole % of total lipid.



(data not shown). The only clear effect on headgroup motion besides temperature itself, is the effect of the gel to liquid-crystalline phase transition temperature as illustrated by the quadrupolar splittings in pure DMPC, which at 10 and 20°C are significantly larger than those for example of DLPC, which at these temperatures is in the fluid phase, or the mixture of DMPC and cholesterol, where the phase transition is abolished by cholesterol (37).

Together the results in Fig. 4 suggest that differences in  $^{14}\text{N}$  quadrupolar splittings when comparing samples at a given temperature well above their phase transition will mostly reflect changes in orientation of the phosphocholine headgroup and not in dynamics. In all forthcoming measurements we therefore use a temperature of 40°C, which is well above the phase transition temperature of the lipids, and we will assume that any change in the  $^{14}\text{N}$  quadrupolar splitting is a direct measure of the change in choline average orientation.

### Effect of charged transmembrane peptides on the PC headgroup orientation

We now have shown that analysis of  $^{14}\text{N}$  quadrupolar splittings is a valuable tool to probe the orientation of the choline headgroup with respect to the bilayer normal and as a response to charges at the lipid/water interface. The next step is to investigate the effect of protein-lipid interactions using designed transmembrane peptides of which the properties can be systematically varied.

KALP23 consists of a hydrophobic sequence of alternating leucines and alanines, flanked at both sides with two lysine residues. The N- and C-terminus are blocked and therefore at neutral pH the peptide contains four positive charges. If these charges at the interface are simply additives, one might expect KALP23 to have a similar effect on headgroup orientation as DMTAP, but at a lipid fraction equivalent to four times the peptide/lipid ratio in the KALP23/PC mixture. As seen in Fig. 5A (and in Table 2), KALP23 indeed affects the  $^{14}\text{N}$  quadrupolar splitting quan-

**TABLE 2** Effect of the inclusion of different peptides on the  $^{14}\text{N}$  quadrupolar splittings (in kHz) of DMPC dispersions as function of the peptide/lipid molar ratio (in mole % peptide)

Mole % peptide	0.5%	1%	2%	3%	4%
Ac-KALP23	10.30	10.19	10.07	10.06	—
KALP23	10.05	9.70	9.12	8.65	8.5
KALP27	—	—	—	8.98	—
KALP31	—	—	—	9.47	—
HALP23 pH4	—	9.11	8.23	—	—
HALP23 pH9	—	10.64	10.63	—	—

titatively similar to that of a fourfold equivalent of DMTAP, pushing the headgroup away from the membrane surface, but only up to 3 mol % of peptide. Above this threshold the effect levels off, possibly because of clustering of the peptides. The effect of KALP23 on the quadrupolar splitting of the DMPC headgroup is in agreement with the work of Roux et al. (38,39), where they show by using  $^2\text{H}$ -NMR that charged peptides are changing the orientation of the choline headgroup in PC bilayers. As a negative control we used an acetylated version of KALP23, in which the integral charges of all four lysine side chains were removed. As expected, the effect of AcKALP23 on the lipid headgroup orientation is very small. Nonetheless, a slight decrease is visible compared to DMPC only. It is possible that this effect arises from another type of interaction such as dipolar interactions from the amide of the acetylated lysine with the polar head of the lipid or it may result from steric hindrance causing the headgroup to be pushed away slightly from the interface.

A perhaps biologically more interesting example of the effect of charges of a transmembrane peptide on the orientation of lipid headgroups would be a pH-sensitive peptide. So far all experiments were carried out at neutral pH. We then used a HALP23 that contains histidines instead of lysines and we varied the pH well beyond the pKa of the histidines. As shown in Fig. 5B, HALP23 has little or no effect on the  $^{14}\text{N}$  quadrupolar splittings at high pH, when the peptide is uncharged, whereas a drastic reduction of the splittings is observed at low pH, when it is positively charged. Interestingly, HALP23 at low pH has a stronger effect than KALP23, suggesting that the low pH used here by itself may have an effect on the quadrupolar splitting, comparable to that of increasing the positive charge density at the bilayer surface. This is rather striking as DMPC is electrostatically neutral and the pH was set relatively far from its pKa, which is around 1 (39). One possibility which would explain this stronger effect of histidine residues at low pH compared to lysines is a strict positioning of the histidine side chains near the phosphate group, whereas the lysine side chain has much more flexibility that could allow it to change its position, perhaps in a more or less similar way as the quaternary ammonium in DMTAP. Although the precise explanation of the relatively large effect of low pH remains unclear, it should be noted that

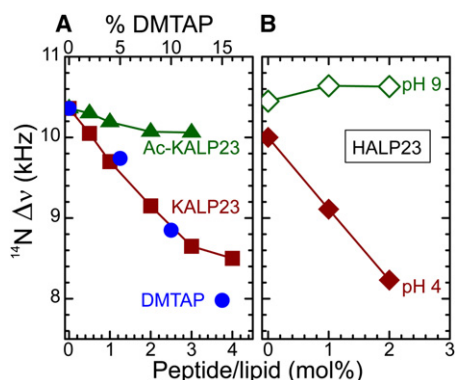


**FIGURE 5** Effect of peptides on the choline head orientation at 40°C. (A) Effect of KALP23 (squares) and its neutral version Ac-KALP23 (triangles), compared to DMTAP (circles). (B) Effect of HALP23 at pH9 (open diamonds) and pH4 (solid diamonds).

Lau and Macdonald (11) observed a similar global reduction of the deuterium order parameter at pH below six when they determined the pKa of membrane bound protein kinase C inhibitor *N,N*-dimethylsphingosine.

These results show that single transmembrane spanning peptides behave in a similar way as other amphiphiles. This is consistent with results of Roux et al. (38) using  $^2\text{H}$  NMR, which showed that a synthetic transmembrane peptide,  $\text{K}_2\text{GL}_{20}\text{K}_2\text{A}$ , with five interfacial positive charges has a strong effect on the orientation of the lipid headgroup. However, it appears inconsistent with the conclusions of Ramamoorthy et al. (22), which to our knowledge, is the only  $^{14}\text{N}$  NMR study published so far on the effect of a membrane-incorporated charged peptide. The authors concluded that the peptide,  $\text{GABA}_A\text{-TM}_2$ , which has two positive charges at the lipid/water interface, has no effect on the  $^{14}\text{N}$  quadrupolar splitting, and hence on the headgroup orientation of PC. A possible explanation for this discrepancy may be linked to the use of oriented samples in this latter study, where important factors such as pH, salts, and hydration cannot be as well controlled as with vesicle suspensions. Another possibility could be that the effect of the charges is influenced by other factors, such as their precise localization with respect to the lipid/water interface.

### Effect of localization of charges at the lipid/water interface

To analyze whether the headgroup orientation is sensitive to the precise location of the charges, we used peptides with a different hydrophobic length. Assuming that the peptides form a regular  $\alpha$ -helix with a translation of 1.5 Å per amino acid, the length of the hydrophobic stretch between the flanking Lys residues would then be 25.5 Å for KALP23, 31.5 Å for KALP27, and 37.5 Å for KALP31. Assuming furthermore a hydrophobic thickness of DMPC of close to 25.4 Å (40), KALP23 would be close to a matching length with a slight positive mismatch, but KALP27 and KALP31 would have a significant positive mismatch and the lysines would be positioned further outward toward the aqueous phase. As shown in the left panel of Fig. 6, even in the situation of a significant positive mismatch, there is still a reduction of the quadrupolar splitting as compared to the situation in the absence of peptide (orange line). Hence, it can be concluded that the longer peptides KALP27 and KALP31 still push the choline away from the membrane surface. This suggests that the lysines in these longer peptides are still localized below the choline moiety of the headgroup. Most probably, at a positive mismatch the lysines only slightly change their localization, because the peptides become tilted or because the lysines preferentially interact with the phosphates and thus remain positioned close to these negatively charged groups. The smaller reduction of the longer peptides as compared to the shorter ones could either be a real effect or it could be an apparent effect related

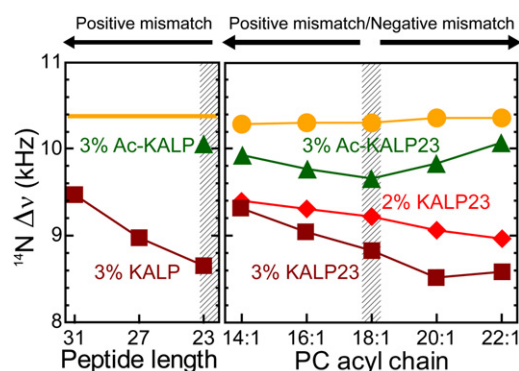


FIGURE 6 Effect of hydrophobic mismatch on the orientation of the choline head. Left panel: Effect of 3 mole % KALP peptides (squares) on DMPC (line) at 40°C as a function of peptide hydrophobic length. The triangle represents the effect of 3 mole % Ac-KALP23. Right panel: Effect of 2 mole % (diamonds), 3 mole % (squares) of KALP23, and 3 mole % Ac-KALP23 (triangles) on the headgroup orientation of varying *cis*-unsaturated PC lipids (circles) at 40°C.

to an increased tendency of the peptides at larger mismatch to self-associate (41,42).

In a complementary experiment (right panel) KALP23 with a fixed length was incorporated into lipids with varying acyl chain length (Table 3). For these experiments unsaturated lipids were used so that the temperature in all cases is far above the liquid-crystalline phase transition temperature. A close to matching situation is now obtained for 18:1-PC (hydrophobic thickness between 26.2 and 26.8 Å (43), and a situation of positive hydrophobic mismatch is achieved by reducing lipid length to 16:1 and 14:1. Both at 3 and 2 mol % of peptide (squares and diamonds in Fig. 6) the quadrupolar splittings of the choline moiety are increased on increasing positive mismatch with the membrane. At extreme negative or positive mismatches, the quadrupolar splittings of the two peptide concentrations appear to converge. Again, this may be a consequence of the increased tendency of the peptides to self-associate at these two extreme mismatched conditions (41,42), reducing the net charge effect.

As a control we tested the effect of the uncharged AcKALP23 at 3 mol %. Here, a small, but significant effect is also observed (triangles), which seems the strongest for matching conditions. This suggests that under these conditions either interaction that may cause these effects such as dipolar interactions are strongest, or that effect on

TABLE 3 Effect of different peptides on the  $^{14}\text{N}$  quadrupolar splittings (in kHz) of various unsaturated PC dispersions

Lipids	14:1-PC	16:1-PC	18:1-PC	20:1-PC	22:1-PC
Lipid only	10.29	10.31	10.31	10.36	10.36
3% Ac-KALP23	9.92	9.76	9.65	9.82	10.07
2% KALP23	9.39	9.3	9.21	9.07	8.97
3% KALP23	9.33	9.06	8.84	8.52	8.59

Peptide percentages represent mole % of peptide.

headgroup orientation by steric hindrance are strongest. Alternatively, the mismatch dependency might be explained by a tendency of the peptide to self-associate under mismatch conditions, as discussed previously.

These results might provide another explanation for the discrepancy with the work of Ramamoorthy et al. (22), who did not observe any effect of incorporation of the cationic peptide GABA<sub>A</sub>-TM<sub>2</sub> on the <sup>14</sup>N NMR spectra of the PC headgroup. This peptide is a transmembrane fragment originating from the pore region of the GABA<sub>A</sub> ionotropic receptor. Despite its positive charges, it will naturally be prone to self-associate even in matching conditions. This will therefore reduce the amount of free positive charges exposed to the PC polar head and hence could explain the absence of a significant effect on the lipid headgroup orientation.

## Lipid mixtures

So far all our data showed the effect of peptides in simple binary mixtures with lipids. We next wanted to find out whether the effects of the peptides on the headgroup of PC remain similar in a slightly more complex environment that better mimics the situation in biological membranes. In terms of interfacial charges the most relevant feature of biological membranes is that they often contain a considerable amount of negatively charged lipids.

Here, we tested the effect of anionic lipids by using mixtures of DMPC and DMPG (Table 4). Advantages of using DMPG are that it has a similar melting temperature as DMPC, preventing any interpretation problem linked to change in overall dynamics of the lipids, and that it contains only one negative charge over a large pH range, making further interpretation easier.

Fig. 7 A shows the effects due to the titration of DMPG on the choline headgroup in DMPC when peptides are added. Open and closed symbols are duplicate, independent experiments, illustrating the reliability of the data. In the absence of peptide (*circles*) the quadrupolar splittings increase with

the amount of anionic lipid, as was already shown in Fig. 3. All peptides shift the response of the headgroup toward the right, thus counteracting the effect of PG on the lipid headgroups. Comparison of the effects of 1 and 2 mol % KALP23 (*diamonds* and *squares*) shows that this effect increases with peptide concentration. However, also acetylated KALP (*triangles*) has a significant effect, possibly due to dipolar interactions or due to steric hindrance, as suggested previously. Surprisingly, the shift in quadrupolar splitting for the charged peptide as compared to the uncharged peptide is significantly larger than expected simply based on charge compensation, because this would result in an offset of 4 and 8 mol% of DMPG only in the case of 1% and 2% of KALP23, respectively.

The same large shift is observed when the quadrupolar splittings are converted to values of PN-angles (Fig. 7 B). Such large shifts may be understood if one would consider the possibility that the KALP peptide does not only make one charged pair with a neighboring DMPG, but preferentially surrounds itself with DMPG. If it would then interact with any of its annular lipids in a similar fashion, i.e., the lysyl group would be hopping between all the surrounding PG lipids, one might expect a shift of ~7 lipids per helix and per monolayer. This would yield to an offset of ~14% DMPG for 1% peptide and twice this amount for 2% peptide.

Fig. 7 C shows that when such a shift is performed for 1% and 2% KALP23, indeed all peptide traces overlay on the neutral peptide Ac-KALP23. For all peptides a rather odd plateau appears between 0% and 20% DMPG after the apparent neutrality is reached, which we do not understand yet. Nonetheless, the slopes before and after the plateau region are similar to the one of the pure lipid system and they are clearly related to the linear change in charge density.

We conclude that the apparent DMPG concentration felt by DMPC is reduced when charged peptides are added, but that the effect seems proportional to the number of annular lipids rather than the amount of charges, suggesting that such a transmembrane peptide is able to cluster

**TABLE 4** Effect of DMPG on the <sup>14</sup>N quadrupolar splittings (in kHz) of DMPC dispersions mixed with peptides

% DMPG	0%	5%	10%	15%	20%	35%	50%	65%	70%	80%	90%
Lipid only (serie 1)	10.37	10.47	10.73	10.92	11.15	11.51	11.72	11.98	—	12.04	—
Lipid only (serie 2)	10.38	10.55	10.60	10.79	10.93	—	11.82	—	12.01	—	12.05
2% Ac-KALP23	10.07	9.95	9.98	10.07	10.23	10.82	11.40	11.63	—	11.80	—
1% KALP23	9.70	9.75	9.95	10.03	9.99	10.28	10.94	11.23	—	11.57	—
2% KALP23 (serie 1)	9.09	9.25	9.37	9.62	9.87	—	10.15	—	10.87	—	11.64
2% KALP23 (serie 2)	9.15	9.34	9.28	9.40	9.71	9.93	10.22	10.77	—	11.17	—
DOPC	11.45	11.09	10.73	10.31	10.13	—	—	—	—	—	—
DLPC	11.61	11.23	10.86	10.51	10.18	9.84	9.53	9.17	—	—	—
DPPC	—	—	—	10.50	10.20	10.00	9.70	9.50	—	—	—
DPPC/ DLPC 8:2	12.04	11.48	10.91	10.42	10.07	9.82	—	—	—	—	—
DMPC pH4	—	—	—	10.00	—	—	—	—	—	—	—
DMPC pH9	—	—	—	10.45	—	—	—	—	—	—	—

Lipid percentages are given as mole percent of DMPG with respect to the total amount of lipid. Peptide percentages represent mole % of peptide.

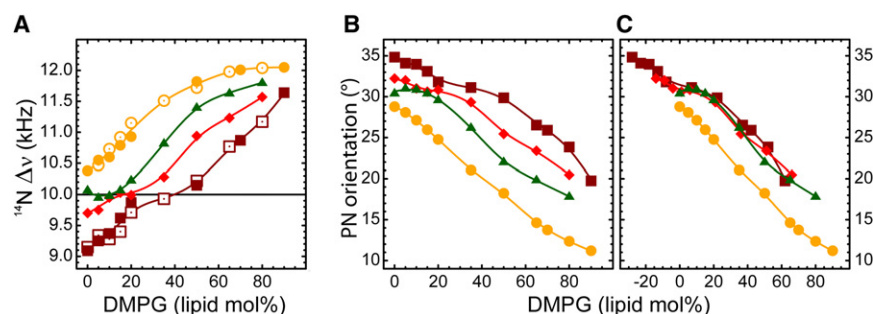


FIGURE 7 (A) Effect of peptides on PC <sup>14</sup>N quadrupolar splittings in mixed DMPC/DMPG bilayers at 40°C: lipid bilayer without peptides (circles); Ac-KALP23 at peptide/lipid ratio (p/l) = 2 mole % (triangles); KALP23 at p/l = 1 mole % (diamonds); and p/l = 2 mole % (squares). Open and closed symbols represent two series of experiments using different batches of lipids and peptide and using a different spectrometer console. (B) Orientation of the P-N vector with respect to the bilayer plane as a function of DMPG in DMPC: lipid only (circles), with 2 mol % Ac-KALP23 (triangles), 1 mole % KALP23 (diamonds), and 2 mole % KALP23 (squares). (C) Same as B except that a fictive % DMPG offset is used (14 lipid mole % and 28 lipid mole % for 1 and 2 mole % of KALP23, respectively).

negatively charged lipids around itself. This would be consistent with results from Franzin and Macdonald on the clustering effect of polylysines on PG in binary mixtures of PC/phosphatidylserine (PS), as analyzed by deuterium NMR (13). Similarly Roux et al (38), using a peptide similar to KALP23, showed by deuterium NMR that in binary mixtures of PC/PS, the lysine has an effect on PS only and not on PC. Thus, those previous observations corroborate our interpretation of the <sup>14</sup>N NMR data presented in this study.

## CONCLUSIONS

To gain insight into general effects of electrostatic interactions between proteins and lipids at the membrane surface, we here exploited the method of <sup>14</sup>N NMR to systematically analyze effects of designed transmembrane peptides on the headgroups of the surrounding lipids in single lipid systems of PC and in binary mixtures of PC and PG. The results show that <sup>14</sup>N NMR analysis of PC is a suitable and robust method to detect subtle changes in headgroup orientation as a consequence of electrostatic interactions. We have successfully demonstrated that it is sensitive to the incorporation of transmembrane peptides and to the localization of the charges. By changing the polar head orientation, the membrane effectively changes its overall thickness and the electric field gradients at its interface. Such changes in turn could affect the interaction of the membrane with membrane-active molecules or they could affect the interaction of the lipids with membrane-embedded proteins. Hence, the orientation and motion of lipid headgroups may play a subtle but decisive role in membrane functioning.

We also could show that negatively charged lipids are attracted by positively charged residues, and that this interaction is directly related to the number of annular lipids, suggesting that negatively charged lipids in proximity of a basic cluster will remain in its vicinity even if no permanent salt bridges are formed. We believe that this result is of prime importance for understanding the role of negatively

charged lipids in the activity and membrane interactions of a variety of membrane proteins, including MscL (44), KcsA (45,46), and phospholamban (47). Future developments could involve refining the approach taken here to model the dynamic behavior of the choline group in more detail, or combining the approach with alternative methods to expand the information on the bilayer structure (48), and to further explore the interactions of membrane-associated peptides and proteins with the lipid bilayer.

This study was supported by a generous grant from the Netherlands Organization for Scientific Research (NWO-TOP grant No. 700-54-303 to J.P.F.D.). B.A.H. was funded by the Biotechnology and Biological Sciences Research Council via the Oxford Centre for Integrative Systems Biology.

## REFERENCES

- Seelig, J., P. M. Macdonald, and P. G. Scherer. 1987. Phospholipid head groups as sensors of electric charge in membranes. *Biochemistry*. 26:7535–7541.
- Jensen, M. Ø., and O. G. Mouritsen. 2004. Lipids do influence protein function—the hydrophobic matching hypothesis revisited. *Biochim. Biophys. Acta*. 1666:205–226.
- Poolman, B., J. J. Spitzer, and J. M. Wood. 2004. Bacterial osmosensing: roles of membrane structure and electrostatics in lipid-protein and protein-protein interactions. *Biochim. Biophys. Acta*. 1666:88–104.
- Marsh, D. 2010. Electron spin resonance in membrane research: protein-lipid interactions from challenging beginnings to state of the art. *Eur. Biophys. J.* 39:513–525.
- Lee, A. G. 2004. How lipids affect the activities of integral membrane proteins. *Biochim. Biophys. Acta*. 1666:62–87.
- Granseth, E., G. von Heijne, and A. Elofsson. 2005. A study of the membrane-water interface region of membrane proteins. *J. Mol. Biol.* 346:377–385.
- Ulmschneider, M. B., and M. S. P. Sansom. 2001. Amino acid distributions in integral membrane protein structures. *Biochim. Biophys. Acta*. 1512:1–14.
- Scherer, P. G., and J. Seelig. 1989. Electric charge effects on phospholipid headgroups. Phosphatidylcholine in mixtures with cationic and anionic amphiphiles. *Biochemistry*. 28:7720–7728.
- Marassi, F. M., and P. M. Macdonald. 1991. Response of the headgroup of phosphatidylglycerol to membrane surface charge as studied by deuterium and phosphorus-31 nuclear magnetic resonance. *Biochemistry*. 30:10558–10566.



10. Marassi, F. M., and P. M. Macdonald. 1992. Response of the phosphatidylcholine headgroup to membrane surface charge in ternary mixtures of neutral, cationic, and anionic lipids: a deuterium NMR study. *Biochemistry*. 31:10031–10036.
11. Lau, B., and P. M. Macdonald. 1995. Determination of the pKa of membrane-bound *N,N*-dimethylsphingosine using deuterium NMR spectroscopy. *Biochim. Biophys. Acta*. 1237:37–42.
12. Macdonald, P. M., K. J. Crowell, ..., D. Semchyschyn. 2000. <sup>2</sup>H NMR and polyelectrolyte-induced domains in lipid bilayers. *Solid State Nucl. Magn. Reson.* 16:21–36.
13. Franzin, C. M., and P. M. Macdonald. 2001. Polylysine-induced <sup>2</sup>H NMR-observable domains in phosphatidylserine/phosphatidylcholine lipid bilayers. *Biophys. J.* 81:3346–3362.
14. Brown, M. F., and J. Seelig. 1977. Ion-induced changes in head group conformation of lecithin bilayers. *Nature*. 269:721–723.
15. Akutsu, H., and J. Seelig. 1981. Interaction of metal ions with phosphatidylcholine bilayer membranes. *Biochemistry*. 20:7366–7373.
16. Siminovitch, D. J., and K. R. Jeffrey. 1981. Orientational order in the choline headgroup of sphingomyelin: a <sup>14</sup>N-NMR study. *Biochim. Biophys. Acta*. 645:270–278.
17. Siminovitch, D. J., M. F. Brown, and K. R. Jeffrey. 1984. <sup>14</sup>N NMR of lipid bilayers: effects of ions and anesthetics. *Biochemistry*. 23:2412–2420.
18. Rothgeb, T. M., and E. Oldfield. 1981. Nitrogen-14 nuclear magnetic resonance spectroscopy as a probe of lipid bilayer headgroup structure. *J. Biol. Chem.* 256:6004–6009.
19. Gally, H.-U., W. Niederberger, and J. Seelig. 1975. Conformation and motion of the choline head group in bilayers of dipalmitoyl-3-sn-phosphatidylcholine. *Biochemistry*. 14:3647–3652.
20. Lindström, F., P. T. F. Williamson, and G. Gröbner. 2005. Molecular insight into the electrostatic membrane surface potential by <sup>14</sup>N/<sup>31</sup>P MAS NMR spectroscopy: nociceptin-lipid association. *J. Am. Chem. Soc.* 127:6610–6616.
21. Sani, M.-A., S. Castano, ..., G. Gröbner. 2008. Restriction of lipid motion in membranes triggered by beta-sheet aggregation of the anti-apoptotic BH4 domain. *FEBS J.* 275:561–572.
22. Ramamoorthy, A., D.-K. Lee, ..., K. A. Henzler-Wildman. 2008. Nitrogen-14 solid-state NMR spectroscopy of aligned phospholipid bilayers to probe peptide-lipid interaction and oligomerization of membrane associated peptides. *J. Am. Chem. Soc.* 130:11023–11029.
23. Killian, J. A., and T. K. M. Nyholm. 2006. Peptides in lipid bilayers: the power of simple models. *Curr. Opin. Struct. Biol.* 16:473–479.
24. Holt, A., and J. A. Killian. 2010. Orientation and dynamics of transmembrane peptides: the power of simple models. *Eur. Biophys. J.* 39:609–621.
25. Kyrychenko, A., M. V. Rodnin, ..., A. S. Ladokhin. 2012. Thermodynamic measurements of bilayer insertion of a single transmembrane helix chaperoned by fluorinated surfactants. *J. Mol. Biol.* 416:328–334.
26. Schäfer, L. V., D. H. de Jong, ..., S. J. Marrink. 2011. Lipid packing drives the segregation of transmembrane helices into disordered lipid domains in model membranes. *Proc. Natl. Acad. Sci. USA*. 108:1343–1348.
27. Nyholm, T. K. M., B. Y. van Duyl, ..., J. A. Killian. 2011. Probing the lipid-protein interface using model transmembrane peptides with a covalently linked acyl chain. *Biophys. J.* 101:1959–1967.
28. de Planque, M. R. R., J.-W. P. Boots, ..., J. A. Killian. 2002. The effects of hydrophobic mismatch between phosphatidylcholine bilayers and transmembrane alpha-helical peptides depend on the nature of interfacially exposed aromatic and charged residues. *Biochemistry*. 41:8396–8404.
29. Kuipers, B. J. H., and H. Gruppen. 2007. Prediction of molar extinction coefficients of proteins and peptides using UV absorption of the constituent amino acids at 214 nm to enable quantitative reverse phase high-performance liquid chromatography-mass spectrometry analysis. *J. Agric. Food Chem.* 55:5445–5451.
30. Rouser, G., S. Fkeischer, and A. Yamamoto. 1970. Two dimensional then layer chromatographic separation of polar lipids and determination of phospholipids by phosphorus analysis of spots. *Lipids*. 5: 494–496.
31. Siminovitch, D. J., M. Rance, ..., M. F. Brown. 1984. The quadrupolar spectrum of a spin *I* = 1 in a lipid bilayer in the presence of paramagnetic ions. *J. Magn. Res.* 58:62–75.
32. Siminovitch, D. J., M. Rance, and K. R. Jeffrey. 1980. The use of wide-line [<sup>14</sup>N]nitrogen NMR as a probe in model membranes. *FEBS Lett.* 112:79–82.
33. Semchyschyn, D. J., and P. M. Macdonald. 2004. Conformational response of the phosphatidylcholine headgroup to bilayer surface charge: torsion angle constraints from dipolar and quadrupolar couplings in bicelles. *Magn. Reson. Chem.* 42:89–104.
34. Williams, T., C. Kelley, ..., J. Zellner. 2011. <http://gnuplot.sourceforge.net/> Accessed September, 2011.
35. Loew, C., K. A. Riske, ..., J. Seelig. 2011. Thermal phase behavior of DMPG bilayers in aqueous dispersions as revealed by <sup>2</sup>H- and <sup>31</sup>P-NMR. *Langmuir*. 27:10041–10049.
36. Brown, M. F., and J. Seelig. 1978. Influence of cholesterol on the polar region of phosphatidylcholine and phosphatidylethanolamine bilayers. *Biochemistry*. 17:381–384.
37. McMullen, T. P. W., and R. N. McElhaney. 1995. New aspects of the interaction of cholesterol with dipalmitoylphosphatidylcholine bilayers as revealed by high-sensitivity differential scanning calorimetry. *Biochem. Biophys. Acta*. 1234:90–98.
38. Roux, M., J.-M. Neumann, ..., M. Bloom. 1989. Conformational changes of phospholipid headgroups induced by a cationic integral membrane peptide as seen by deuterium magnetic resonance. *Biochemistry*. 28:2313–2321.
39. Moncelli, M. R., L. Becucci, and R. Guidelli. 1994. The intrinsic pKa values for phosphatidylcholine, phosphatidylethanolamine, and phosphatidylserine in monolayers deposited on mercury electrodes. *Biophys. J.* 66:1969–1980.
40. Kučerka, N., Y. Liu, ..., J. F. Nagle. 2005. Structure of fully hydrated fluid phase DMPC and DLPC lipid bilayers using X-ray scattering from oriented multilamellar arrays and from unilamellar vesicles. *Biophys. J.* 88:2626–2637.
41. Sparr, E., W. L. Ash, ..., J. A. Killian. 2005. Self-association of transmembrane alpha-helices in model membranes: importance of helix orientation and role of hydrophobic mismatch. *J. Biol. Chem.* 280:39324–39331.
42. Ren, J., S. Lew, ..., E. London. 1999. Control of the transmembrane orientation and interhelical interactions within membranes by hydrophobic helix length. *Biochemistry*. 38:5905–5912.
43. Pan, J., S. Tristram-Nagle, ..., J. F. Nagle. 2008. Temperature dependence of structure, bending rigidity, and bilayer interactions of dioleoylphosphatidylcholine bilayers. *Biophys. J.* 94:117–124.
44. Powl, A. M., J. M. East, and A. G. Lee. 2008. Anionic phospholipids affect the rate and extent of flux through the mechanosensitive channel of large conductance MscL. *Biochemistry*. 47:4317–4328.
45. Marius, P., M. Zagnoni, ..., A. G. Lee. 2008. Binding of anionic lipids to at least three nonannular sites on the potassium channel KcsA is required for channel opening. *Biophys. J.* 94:1689–1698.
46. van Dalen, A., and B. de Kruijff. 2004. The role of lipids in membrane insertion and translocation of bacterial proteins. *Biochim. Biophys. Acta*. 1694:97–109.
47. Li, J., Z. M. James, ..., D. D. Thomas. 2012. Structural and functional dynamics of an integral membrane protein complex modulated by lipid headgroup charge. *J. Mol. Biol.* 418:379–389.
48. Gan, Z., P. L. Gor'kov, ..., C. P. Grey. 2009. Enhancing MQMAS of low- $\gamma$  nuclei by using a high B(1) field balanced probe circuit. *J. Magn. Reson.* 200:2–5.